The role of imaging modalities in diagnostics of posterior paravertebral mediastinal pathologic changes

Dovilė Barakauskaitė[1], Simas Giedrys[1], Ieva Keturkaitė[1], Kamilė Pocepavičiūtė[1], Laima Dobrovolskienė[1]

[1] *Department of Radiology of Lithuanian University of Health Sciences Kaunas, Lithuania.*

ABSTRACT

Background: Different paravertebral pathologies in posterior mediastinum may cause diagnostic difficulties. Usually, the symptoms are not specific, and the changes are found during routine investigations. In roentgenograms, they do not have specific features so more accurate imaging modality must be chosen to define whether it is benign or malignant. This can be made by using a CT or MRI scan. It is crucial to choose the right strategy for each pathology, as the aim of imaging may vary in different situations. The aim of our study was to evaluate and compare the features of pathological findings in the posterior mediastinum.

Materials and methods: We performed the retrospective observational study at LUHS hospital Kauno Klinikos Radiology clinic. Medical health records and x-ray, CT and MRI radiologic view made between 2015 and 2019 were analyzed. Patients who underwent CT and MRI scanning repeatedly for clarification of diagnosis were investigated PET/CT or were operated for histological confirmation of diagnosis and who had pathologic findings in posterior mediastinum were selected.

Results: The study consisted of 81 patients with verified posterior mediastinal masses. A variety of clinical diagnoses were confirmed, 70,4% (n = 57) of the masses were oesophagal tumours, and the remaining cases consisted of benign cysts and other cysts like lesions. Oesophagal tumours were most commonly located in the middle thoracic part of the oesophagus and presented itself as a circular wall thickening with a homogenous structure and a rare rate of local invasion of adjacent structures. There was a statistically significant difference between attenuation on CT scan before and after the administration of intravenous contrast medium (p<0,001). The majority of cystic masses 66,7% (n=16) presented with a well-defined circumscribed border on a conventional radiograph. CT images showed that 79,2% (n=19) masses were heterogeneous and had a various degree of contrast enhancement. In diffusion-weighted magnetic resonance imaging, ADC values was measured with an average of 1,86 0,99 * 10-3mm2/s. PET/CT showed hypermetabolism in 41,7% (n=10) of the masses and possibly benign, no metabolic changes in the remaining 58,3% (n=14). There was no statistically significant difference in mean attenuation measured on CT between metabolically active and inactive masses (p=0,546). There was a statistically significant difference in apparent diffusion coefficient between metabolically active and inactive masses (p=0,005).

Conclusion: Conventional chest radiography can be helpful to define the anatomical location, borders and size of the masses. Multislice computed tomography can help to obtain information about densities and CE of the lesion. In different sequences of MRI masses have an isointense or hyperintense signal which provides additional information about the inner structure of lesion. Apparent diffusion coefficient (ADC) in MRI can be helpful distinguishing malignant from benign masses.

Keywords: computed tomography, magnetic resonance imaging, posterior mediastinum

INTRODUCTION

Posterior mediastinum is the anatomical region that contains a variety of structures such as the descending thoracic aorta, oesophagus, azygos and hemiazygos veins, thoracic duct, lymph nodes, adipose tissue, vagus and splanchnic nerves, and autonomic ganglia. Due to this, the range of pathologies in this region may be broad. Masses of the mediastinum are usually found incidentally during routine chest investigations [1]. In roentgenograms, they appear as rounded lesions with increased opacity, and 40.7% of cases are asymptomatic [1]. Symptoms arise from the compression on mediastinal structures, but they are not specific. These include dyspnea, chest pain, cough and dysphagia [1].

The main goal of investigating these cases is to

identify whether the mass in the posterior mediastinum is malignant or benign. If the process is malignant, the aim is to determine the stage. In the case of the benign process, the most important is to choose the right strategy for observing the changes during the time. Such imaging modalities as CT and MRI scan can precisely specify the localization, size, tissue characteristics and relationship with other structures.
The aim of this study was to evaluate and compare CT and MRI findings of malignant and benign pathologies in the posterior mediastinum.

BRONCHOGENIC CYSTS

Posterior mediastinum is one of the regions where bronchogenic cysts may appear [2]. In 52% of cases, they are located near carina [4]. These cysts contain mucous gland tissue and muscle [3]. The size may increase due to haemorrhage or infection [3].
On chest radiographs, they usually appear as well-defined solitary masses with homogenous opacity [2]. On CT scans, bronchogenic cysts appear as sharply marginated mediastinal masses with attenuation value varying from water to soft-tissue attenuation [5]. MRI can help to sort out the nature of cystic lesion [5]. The appearance of fluid-fluid levels seen on MRI can help to confirm the true cystic nature of bronchogenic cyst [6].

MATURE CYSTIC TERATOMA

Mature cystic teratoma is a cystic tumour that may contain skin, teeth, hair, bone, cartilage and even bronchial or gastrointestinal epithelium [2]. Only 3%-8% of these cysts are in the posterior mediastinum, while a majority of them appears in anterior mediastinum [26]. On plain chest films, they appear as sharply marginated, round or lobulated masses that extend to the one side of the midline [2]. Ossification, calcification and teeth may be apparent [7]. On CT, they are well-defined heterogeneous masses with the walls that may enhance the contrast [8]. Fluid, fat, soft tissue and calcium may be apparent [8]. On MRI, they appear as heterogeneous masses containing the same kinds of tissues, as mentioned before [9].

INTRATHORACIC MENINGOCELE

Intrathoracic meningocele is a cystic sac in the thoracic cavity that contains cerebral fluid and is formed by spinal meninges. These cystic lesions are associated with neurofibromatosis [10]. Patients without neurofibromatosis rarely develop these kinds of cysts [11].
At radiography, they present as sharply defined round, lobulated or smooth paraspinal masses [2]. At CT, intrathoracic meningoceles appear as well-defined, homogenous, low-attenuation paravertebral masses [2]. On MRI, it appears as a cystic mass with homogenous structure and connection with the spinal canal [11]. The intensity of cystic mass is similar to cerebrospinal fluid on T2 weighted images [11].

LYMPHANGIOMA

Lymphangioma is a congenital benign lesion. It is caused by the focal proliferation of lymphatic tissue with a multicystic pattern [12]. Only 10% of manifest in the thorax; meanwhile it is prevalent in the axillary region and neck [13]. Due to their soft consistency, the symptoms are rare [2]. At radiography, they usually appear as well-defined, round, lobulated masses [14]. Pleural effusions may present as well, and they may be unilateral or bilateral [2]. On CT, they usually appear as smooth lobulated mass [14]. They can have both low and high attenuation, depending on cystic content [2].
On MRI, at T1-weighted images, they have similar or higher signal than muscle [15]. On T2-weighted images, high signal intensity is characteristic due to the cystic substance [15].

NEURENTERIC CYST

Neurenteric cysts are rare and may have a connection with meninges [14]. They are composed of heterotopic endodermal tissue and are associated with abnormalities of the spine [16]. The symptoms usually appear due to the compression of the spinal cord and associated nerve roots [16]. CT is suitable for evaluating vertebral abnormalities. However, MRI is superior in defining the nature of these structures [17]. MRI findings are isointense lesions in T1-weighted

images and hyperintense lesions on T2-weighted images [18]. Also, MRI is the most suitable imaging modality for long-term follow-up as the recurrence is characteristic [17]. MRI is accepted to be the gold standard for defining neurenteric cysts [16].

CYSTLIKE LESIONS

Some of the pathologies may go through cystic degeneration and appear as mixed cystic and solid structures on CT and MRI [2]. In general, these changes include Hodgkin disease, mediastinal carcinomas, malignant lymphoma and metastases [2, 19, 20]. Radiation therapy and chemotherapy may induce these lesions [2]. On CT, cystic changes have low attenuation, complex structure with a fluid like areas [20]. However, in some cases, findings may be equivocal, and diffusion MRI technique may be useful in differentiating between malignant and benign pulmonary masses [21]. The conclusion can be made by calculating the mean apparent diffusion coefficient (ADC) value [22]. The sensitivity of this technique is 90% and specificity - 100% [22]. Greater than 5mm nodules can be differentiated while using ADC value as well [23].

OESOPHAGAL TUMORS

Adenocarcinoma and squamous cell carcinoma are the most common types of oesophagal cancer. At an early stage, it may be asymptomatic. Tumour extension to mediastinum can cause chest pain. The first method for diagnosing oesophagal cancer is endoscopy with biopsy. CT scan is the modality of choice to determine TNM staging, and it helps diagnose local mediastinal invasion [24]. MRI is not routinely used for oesophagal cancer staging though it has potential to improve staging [25].

METHODS AND MATERIALS

We performed a retrospective observational study at Kaunas Clinics. Kaunas Regional Biomedical Research Ethics Committee (KRBRE) approved the study protocol and waived informed consent. In this study, medical health records made between 2015 and 2019 were analyzed. We selected patients medical records who underwent X-ray, CT and MRI scan for suspected posterior mediastinal pathology. CT scans were performed with Toshiba Aquilion One 320 slice equipment, using 120 kV, high resolution scanning with 0,5 mm slice thickness. Before the oesophagal part was scanned, the patient had to take 50 - 100 ml contrast medium per orally, and the other had intravenous contrast material. MRI scans were performed using 1.5T (Siemens Aera) or 3T (Philips Ingenia) scanners. VIBE, HASTE, BLADE TIRM, STIR sequences were used. The gold standard for diagnosis were PET/CT conclusion, histological confirmation or absence changes of the benign lesion in repeatedly CT or MRI view. Description of CT, MRI and PET/CT scans were reviewed and compared retrospectively from the medical health records. Statistical analysis of selected data was performed using "Microsoft® Excel" and statistical package "SPSS for Windows 26.0". Descriptive statistics are provided by the mean and standard deviation (M ± SD) or percentages. The distribution of quantitative traits, according to the Gaussian distribution, was checked using the Shapiro-Wilk or Kolmogorov-Smirnov criteria. The averages of the two dependent samples were compared using Student's T criteria. Differences between two independent samples were compared using the Mann-Whitney U Test.

RESULTS

1) Demographic and clinical characteristics

The study consisted of 81 patients with verified posterior mediastinal masses. The majority of participants, 74,1% (n = 60) were male and 25,9% (n = 21) were female, with a male:female ratio of 2,86:1. Patient's age ranged from 28 to 88 with the average age of 62,52 12,14. A variety of clinical diagnoses were confirmed, 70,4% (n = 57) of the masses were esophageal tumors out of which 89,5% (n = 51) were squamous cell carcinoma, 8,8% (n = 5) adenocarcinoma and 1,8% (n=1) primary melanoma of the esophagus. 29,6% (n = 24) of the cases consisted of benign cysts and other cyst like lesions. By origin 20,8% (n = 5) of the cysts were bronchogenic, 8,3%(n= 2) were neurenteric cysts, 8,3%(n= 2)

cases were confirmed as mature cystic teratoma, 4,2% (n = 1) as meningocele and 4,2% (n = 1) as lymphangioma. 54,2% (n = 13) were other cyst like lesions, which were identified by histological examination as neurogenic tumors, primary pulmonary adenocarcinoma, lymphoma, hemartoma and distant metastases.

2) Computed tomography imaging of oesophagal tumours

All of the patients who were diagnosed with oesophagal tumours had undergone chest and abdominal CT examination. Mean thickness of the oesophagus wall was measured 15,39 7,17mm, and mean tumour length was 6,34 2,66cm. The average attenuation (Hounsfield Units) before the administration of intravenous contrast medium was 30,8 10,31 Hu, and after intravenous contrast medium was injected, the average attenuation was 65,68 24,25 Hu. (Fig 1.)

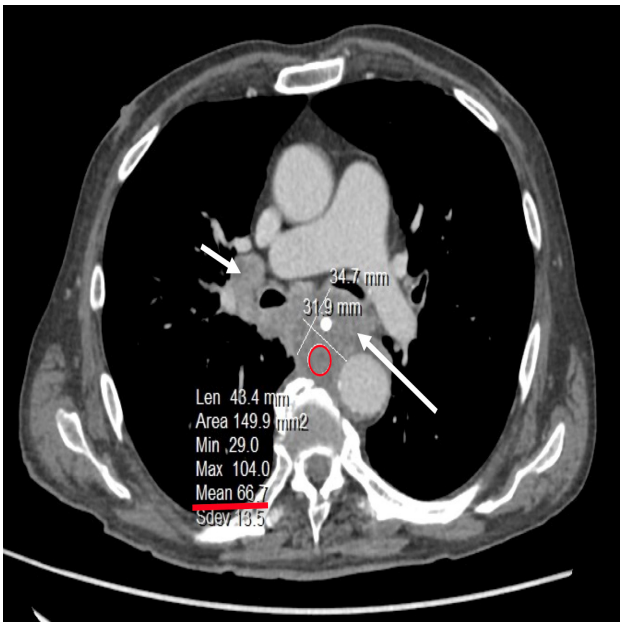

Fig.1 51-year patient's CT axial slice with CE demonstrate pathologic oesophagal masses and pathologic lymph nodes conglomerate below bifurcation (arrows). ROI (red ring) shows mean of attenuation 66,7 Hu after CE.

There was a statistically significant difference between attenuation before and after the administration of intravenous contrast medium ($p<0,001$).

The examination of CT images showed circular oesophagal wall thickening in 57,9% (n=33) of the cases and asymmetrical, eccentric thickening in remaining 42,1% (n=24) cases. The fat stranding was seen in 61,4 (n=35) of the cases. The majority 77,2% (n=44) of oesophagal masses had homogenous structure; however, after the administration of intravenous contrast medium 52,6% (n=30) showed nonhomogeneous enhancement of the tumour. The most common location of squamous cell carcinoma was the middle thoracic oesophagus, and adenocarcinoma was most prevalent in the lower part of the thoracic oesophagus (Fig. 1). 14,04% of the cases showed evident local invasion of adjacent structures with 75% (n=6) being a tracheobronchial tree and 25% (n=2) invasion into the aorta.

Fig 2. Location and histology of oesophagal masses

Location	Squamous cell carcinoma		Adenocarcinoma	
	n	%	n	%
Upper thoracic part	9	17,65%	0	0
Middle thoracic part	26	50,98%	1	20%
Lower thoracic part	16	31,37%	4	80%

3) The multimodal approach to imaging of cystic posterior mediastinal masses

A conventional frontal and lateral chest radiograph was performed for 29,6% (n = 24) of patients and examined to determine the anatomical location, borders and size of the masses. The mean diameter of the masses was 4,87 2,26cm with a minimum of 1,5cm and maximum of 9,2cm. The majority of the masses 66,7% (n=16) presented with a well-defined circumscribed border, and remaining cases showed sharply marginated, ill-defined borders (Fig.3)

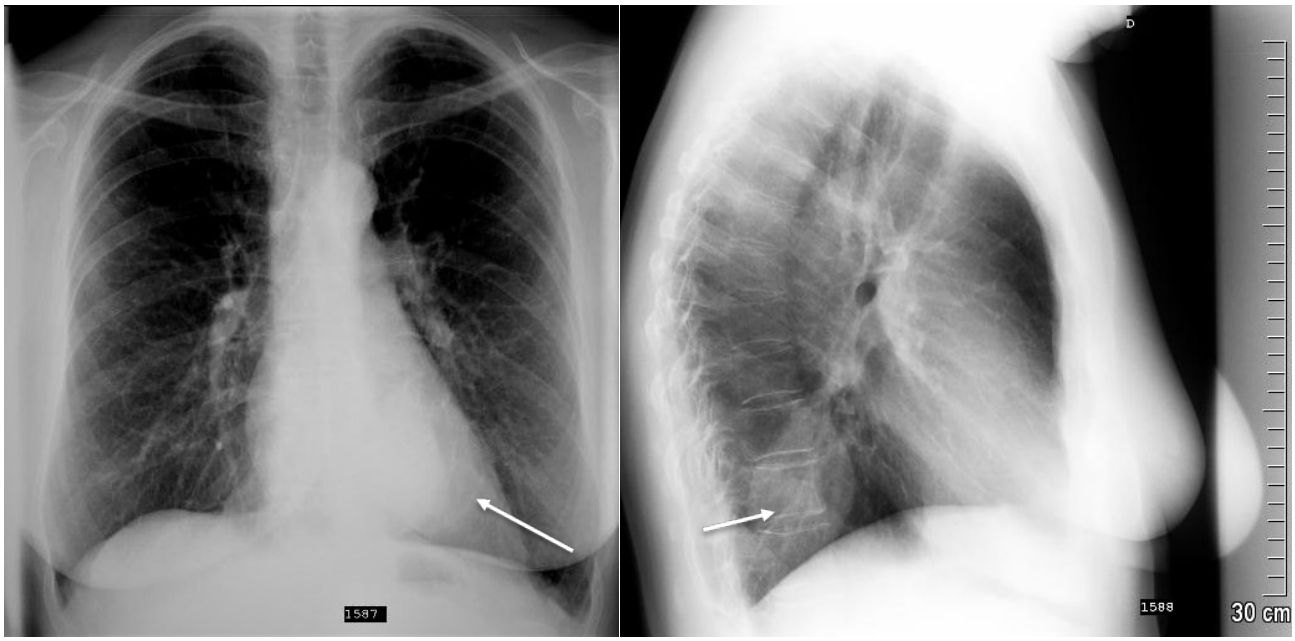

Fig.3 29-year patient's chest PA (a) and lateral (b) x-rays demonstrate (arrows) left lower paravertebral ill-defined pathologic masses.

Fig 4. Location of cystic masses by side and segment of the masses epicentre

Location	segment 1		segment 2		segment 3	
Left side	9	37,5%	0	0%	3	12,5%
Right side	7	29,17%	5	20,83%	0	0%

Multislice computed tomography and magnetic resonance imaging scan were performed to obtain more detailed information. CT images showed that 79,2% (n=19) masses had heterogeneous structure and 20,8% (n=5) were homogenous. After administration of intravenous contrast medium, 33,3% (n=8) showed no enhancement and had mean attenuation of 47,25 7,72Hu. 20,8% (n=5) masses showed slight enhancement, 29,2% (n=7) borderline enhancement and 16,7% (n=4) showed intense enhancement with average attenuation of 48 4,19Hu (Fig.5).

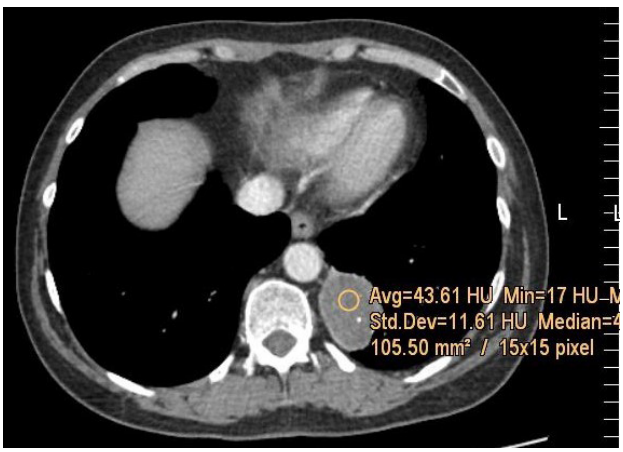

Fig.5. 29-year patient's CT axial scan after CE demonstrate (arrow) left paravertebral ill-defined homogeneous cystic lesions with 43 HU attenuation (ROI).

MRI HASTE sequence showed signal isointensity in 45,8% (n=11) of the cases, hyperintensity in 54,2% (n=13) and not a single case of hypointense signal when compared to muscle tissue signal (Fig.6). MRI TIRM sequence showed signal hypointensity in 25% (n=6), isointensity in 37,5% (n=9) and hyperintensity in 37,5% (n=9). In diffusion-weighted magnetic resonance imaging apparent diffusion coefficient (ADC) was measured with an average of 1,86 0,99 x10-3mm2/s with a minimal value of 0,8 x 10-3 mm2/s and maximum value of 3,6 x 10-3mm2/s (Fig.7 a,b).

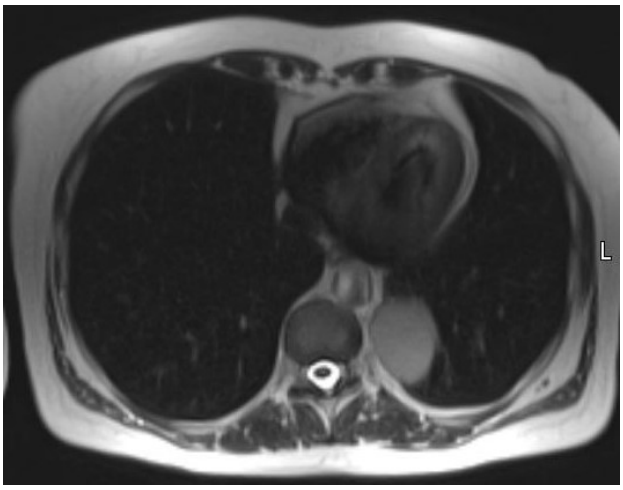

Fig.6. 29-year patient's HASTE axial MRI view shows signal hyperintensity in the oval left paravertebral lesion (arrow).

Fig.7. 29-year patient's MRI TIRM coronal (a) view shows (arrow) signal hypointensity in oval left paravertebral lesion, and DWI axial slice ROI shows high 2,1 x 10-3mm2/s ADC.

Positron emission tomography-computed tomography (PET/CT) was also performed for the aforementioned patients showing hypermetabolism in 41,7% (n=10) of the masses and no metabolic changes in the remaining 58,3% (n=14).

There was no statistically significant difference in mean attenuation measured on CT between metabolically active and inactive masses (p=0,546). There was a statistically significant difference in apparent diffusion coefficient between metabolically active and inactive masses (p=0,005).

DISCUSSION

Masses of the posterior mediastinum are usually found incidentally during routine chest investigations, and in most of the cases, they appear as rounded, sharply marginated lesions [1, 2]. In this study, we found that the majority of the posterior paravertebral masses 66,7% (n=16) presented with a well-defined circumscribed border, and remaining cases showed sharply marginated ill-defined borders. These

Fig 8. The difference between ADC value by metabolic activity

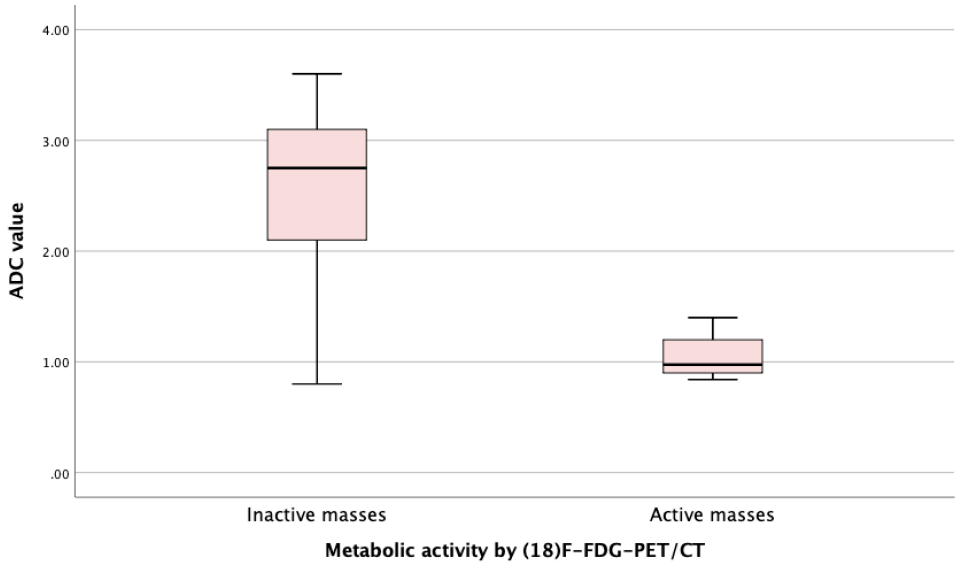

findings were not specific, so more precise imaging modalities were used.

We predicted that the nature of the mass could be distinguished by using a CT or MRI scan.

On CT, they can have both low and high attenuation, depending on cystic content [2]. Intrathoracic meningoceles and cystlike lesions have low attenuation [2, 20]. Bronchogenic cysts, lymphangiomas can have both low and high attenuation [2, 5]. Fluid, soft tissue, fat or calcium may be apparent in the case of mature cystic teratoma [8]. Cystlike lesions may have a complex structure with a fluid like areas [20]. As a result, imaging findings are similar in some types of paravertebral masses, so only the attenuation, structure, content and relation with other structures can be assessed. In the present study, CT images showed that the majority of cystic masses 79,2% (n=19) had heterogeneous structure, 33,3% (n=8) showed no enhancement and the remaining masses showed a various degree of enhancement with no significant difference of mean attenuation between the two, showing similarities to a study by K. Pulasani et al. that displayed heterogeneous enhancement in the majority (44%) of the tumours, no enhancement in 28% of the masses and no significant differences between structural characteristics and malignancy [30]. However, relying just on these findings, we cannot conclude in determining whether the mass is malignant or benign.

Correspondingly to a study by Chandna P et al. that showed 64% of oesophagal tumours were homogenous on CT scan, in our study the majority 77,2% (n=44) of oesophagal masses also had homogenous structure, however, after the administration of intravenous contrast medium 52,6% (n=30) showed nonhomogeneous enhancement [27]. When comparing malignant oesophagal tumours, there was a statistically significant difference between attenuation before and after the administration of intravenous contrast medium ($p<0,001$) similarly to a study by Abbey J. Winant et al. [28].

MRI can help to confirm the cystic nature of the mass [6]. This imaging modality is beneficial for long-term follow-ups, as well [17]. The diagnosis of a benign or malignant process can be made by calculating the mean apparent diffusion coefficient (ADC) value [22]. Tondo et al. reported that the sensitivity of this technique is 90% and specificity - 100% [22]. In our study, we found a statistically significant difference of apparent diffusion coefficient between metabolically active masses 1,05 0,06 x 10-3mm2/s and inactive masses 2,45 0,24 x 10-3mm2/s ($p=0,005$), equivalently to a study by Shin K.E. that got the same results with mean averages of 1.46 ± 0.50 x 10-3mm2/s and 3.67 ± 0.87 x 10-3mm2/s respectively [29].

CONCLUSIONS

A wide range of diagnostic methods can be used to diagnose paravertebral mediastinal pathologies. In our study, we concluded that conventional chest radiography could be helpful to define the anatomical location, borders and size of the masses. Multislice computed tomography can help to obtain information about densities and CE of the lesion. In MRI different sequences, the masses have an isointense or hyperintense signal which provides more information about the inner structure of lesion. Apparent diffusion coefficient (ADC) in MRI can be helpful distinguishing malignant from benign masses.

REFERENCES

1. Osama Saber Eldib, Abdelmeged Salem. Surgical management of mediastinal cysts, Journal of the Egyptian Society of Cardio-Thoracic Surgery, Volume 24, Issue 1, 2016. https://doi.org/10.1016/j.jescts.2016.03.001

2. Mi-Young Jeung, Bernard Gasser, Afshin Gangi, et al. Imaging of Cystic Masses of the Mediastinum. RadioGraphics 2002 22:suppl_1, S79-S93 https://pubs.rsna.org/doi/10.1148/radiographics.22.suppl_1.g02oc09s79

3. Juanpere, S., Cañete, N., Ortuño, P. et al. A diagnostic approach to the mediastinal masses. Insights Imaging 4, 29–52 (2013). https://doi.org/10.1007/s13244-012-0201-0

4. Takahashi K, et al. Computed tomography and magnetic resonance imaging of mediastinal tumors. J Magn Reson Imaging. 2010;32:1325–1339. doi: 10.1002/jmri.22377.

5. McAdams HP, Kirejczyk WM, Rosado-de-Christenson ML, et al. Bronchogenic cyst: imaging features with clinical and histopathologic correlation. Radiology. 2000;217:441-6.

6. Lyon RD, McAdams HP. Mediastinal bronchogenic cyst: demonstration of a fluid-fluid level at MR imaging. Radiology 1993; 186:427-428.

7. Moeller KH, Rosado-de-Christenson ML, Templeton PA. Mediastinal mature teratoma: imaging features. AJR Am J Roentgenol 1997; 169:985-990.

8. Tecce PM, Fishman EK, Kuhlman JE. CT evaluation of the anterior mediastinum: spectrum of disease. RadioGraphics 1994; 14:973-990.

9. Brown LR, Aughenbaugh GL. Masses of the anterior mediastinum: CT and MRI findings. AJR Am J Roentgenol 1991; 157:1171-1180.

10. Gocer AI, Tuna M, Gezercan Y et al. Multiple anterolateral cervical meningoceles associated with neurofibromatosis, Neurosurg Rev, 1999, vol. 22 (2–3)(pg. 124-126)

11. Mehmet Turgut, Cumhur Alhan, Mutlu Cihangiroglu, Mehmet Sah Topcuoglu, Isolated giant intrathoracic meningocele associated with vertebral corpus deformity, Interactive CardioVascular and Thoracic Surgery, Volume 3, Issue 2, June 2004, Pages 381–383, https://doi.org/10.1016/j.icvts.2004.02.009

12. Vilela, Tiago Tavares, Daher, Renato Tavares, Nóbrega, Mariana Domiciano Albuquerque, Ximenes Filho, Carlos Alberto, Montandon, Cristiano, & Montandon Júnior, Marcelo Eustáquio. (2009). Congenital mediastinal cysts: imaging findings. Radiologia Brasileira, 42(1), 57-62. https://doi.org/10.1590/S0100-39842009000100012

13. Charruau L, et al. Mediastinal lymphangioma in adults: CT and MRI imaging features. Eur Radiol. 2000;10:1310–1314. doi: 10.1007/s003300000380.

14. Ödev K, Arıbaş BK, Nayman A, Arıbaş OK, Altınok T, Küçükapan A. Imaging of cystic and cystlike lesions of the mediastinum with pathologic correlation. J Clin Imaging Sci 2012; 2: 33.

15. Shaffer K, Rosado-de-Christenson ML, Patz EF, Jr, Young S, Farver CF. Thoracic lymphangioma in adults: CT and MR imaging features. AJR Am J Roentgenol. 1994;162:283–9.

16. Savage J, Casey J, McNeill I, et al. Neurenteric cysts of the spine. J Craniovertebr Junction Spine. 2010;1(1):58.

17. Brooks BS, Duvall ER, el Gammal T, Garcia JH, Gupta KL, Kapila A. Neuroimaging features of neurenteric cysts: Analysis of

nine cases and review of the literature. AJNR Am J Neuroradiol. 1993;14:735–46.

18. Menezes AH, Traynelis VC. Spinal neurenteric cysts in the magnetic resonance imaging era. Neurosurgery. 2006;58:97–105. discussion 97-105.

19. Youssriah Yahia Sabri, Mona Ahmed Fouad, Hebata-Allah Hany Assal, Hassan Ebrahim Abdullah. Cystic lesions in multi-slice computed tomography of the chest: A diagnostic approach. The Egyptian Journal of Radiology and Nuclear. Medicine, Volume 47, Issue 4, 2016.

20. K.D. Hopper, L.F. Diehl, M.A. Cole, J.C. Lynch, J.W. Meilstrup, M.A. McCauslin. The significance of necrotic mediastinal lymph nodes on CT in patients with newly diagnosed Hodgkin disease. Am J Roentgenol, 155 (6) (1990), pp. 267-270

21. Razek AA. Diffusion magnetic resonance imaging of chest tumors. Cancer Imaging. 2012;12(3):452–463. Published 2012 Oct 26. doi:10.1102/1470-7330.2012.0041

22. Tondo F, Saponaro A, Stecco A, et al. Role of diffusion-weighted imaging in the differential diagnosis of benign and malignant lesions of the chest–mediastinum. Radiol Med. 2011;116:720–733. doi: 10.1007/s11547-011-0629-1. . PMid:21293944.

23. Satoh S, Kitazume Y, Ohdama S, Kimula Y, Taura S, Endo Y. Can malignant and benign pulmonary nodules be differentiated with diffusion-weighted MRI? Am J Roentgenol. 2008;191:464–470. doi: 10.2214/AJR.07.3133.

24. van Vliet EPM, Heijenbrok-Kal MH, Hunink MGM, Kuipers EJ, Siersema PD. Staging investigations for oesophageal cancer: a meta-analysis. Br J Cancer2008;98:547-57.doi:10.1038/sj.bjc.6604200 pmid:18212745

25. van Rossum PS, van Hillegersberg R, Lever FM, et al. Imaging strategies in the management of oesophageal cancer: what's the role of MRI? Eur Radiol. 2013;23:1753–1765.

26. Rosado-de-Christenson ML, Templeton PA, Moran CA. From the archives of the AFIP. Mediastinal germ cell tumors: radiologic and pathologic correlation. RadioGraphics 1992; 12:1013-1030.

27. Chandna P, Siddesh MB, Jeevika MU, Kochar PKT. CT imaging and staging of carcinoma oesophagus. Int J Res Med Sci 2017;5:2021-9.

28. Abbey J. Winant, Marc J. Gollub, Jinru Shia, Christina Antonescu, Manjit S. Bains, and Marc S. Imaging and Clinicopathologic Features of Esophageal Gastrointestinal Stromal Tumors. Levine American Journal of Roentgenology 2014 203:2, 306-314

29. Shin, K.E., Yi, C.A., Kim, T.S. et al. Diffusion-weighted MRI for distinguishing non-neoplastic cysts from solid masses in the mediastinum: problem-solving in mediastinal masses of indeterminate internal characteristics on CT. Eur Radiol 24, 677–684 (2014). https://doi.org/10.1007/s00330-013-3054-0

30. Kireet Pulasani , Indira Narayanaswamy , H V Ramprakash. Evaluation of Mediastinal Mass Lesions Using Multi-detector Row Computed Tomography and Correlation with Histopathological Diagnosis. International Journal of Scientifi c Study. Volume 3, Issue 6, Sep 2015.